RSC Advances

PAPER

View Article Online
View Journal | View Issue

Cite this: *RSC Adv.*, 2026, **16**, 20131

Room-temperature chemiresistive CO detection by PANi/GO nanocomposite sensors

Imash Aigerim, [abc] Smagulova Gaukhar, [*acd] Kazhdanbekov Ramazan, [b] Kaidar Bayan, [e] Efremov Vladimir [a] and Mansurov Zulkhair [ab]

Received 23rd November 2025
Accepted 11th April 2026

DOI: 10.1039/d5ra09053a

rsc.li/rsc-advances

Against the backdrop of growing environmental and industrial risks, particularly those associated with toxic CO emissions, the development of highly sensitive gas sensors capable of operating stably at room temperature is of strategic importance. This work investigates composite materials based on polyaniline (PANi) and graphene oxide (GO) as promising sensing elements for carbon monoxide (CO) detection. It was found that pristine PANi exhibits limited gas sensitivity, yielding a response of only 9.7% upon CO exposure. The introduction of GO into the polymer matrix facilitates the formation of conductive pathways, increases the number of active adsorption sites, and accelerates charge transfer processes, resulting in a pronounced synergistic effect. Consequently, the PANi/GO composite achieves a response of 31.5%, which is nearly three times higher than that of pure PANi. A detailed comparative analysis indicates that the carbon nanostructures play a dual role: they enhance the conductivity of the system and activate surface gas–material interactions. Thus, the formation of hierarchical composites based on PANi and GO represents an effective strategy for enhancing the sensitivity and improving the dynamic characteristics of room-temperature CO sensors. The obtained results confirm the high potential of PANi/GO composites for applications in environmental monitoring systems, industrial safety, and next-generation intelligent sensor platforms.

Introduction

The rapid expansion of urban agglomerations, accompanied by increasing transportation and industrial activity, has led to a systematic deterioration in ambient air quality. Among the most hazardous components of anthropogenic emissions is carbon monoxide (CO), a colorless and odorless gas exhibiting high toxicity even at low concentrations. Its formation is typically associated with the incomplete oxidation of hydrocarbon fuels in internal combustion engines, heating systems, and industrial units.[1–4] The danger of CO arises from its biochemical interaction with hemoglobin: its markedly high affinity for Fe^{2+} centers-200–250 times greater than that of oxygen-results in the formation of stable carboxyhemoglobin, which inhibits oxygen transport and induces systemic hypoxia.[5] Even short-term exposure to 20–30 ppm of CO may lead to dizziness and impaired cognitive function, whereas concentrations above 150–200 ppm pose an immediate threat to life.[6] According to the WHO, a significant proportion of the global population is regularly exposed to CO levels exceeding permissible limits, a situation further aggravated by the presence of co-emitted pollutants such as methane, volatile organic compounds, and nitrogen oxides.[7,8]

The growing challenges associated with environmental monitoring underscore the need for highly sensitive sensing systems capable of detecting CO at low operating temperatures and minimal power consumption. Gas sensors are currently employed across a broad range of fields-from environmental surveillance and industrial safety to medical diagnostics, geophysical studies, and analytical control of air and water composition.[9,10] Existing detection techniques include nondispersive infrared spectroscopy,[8] catalytic combustion,[11] surface acoustic wave sensors,[12] and semiconductor-based sensing platforms[13] including modern electrochemical approaches for the detection of toxic gases and related analytes, based on the use of catalytically active and nanostructured materials, encompassing both chemical sensors[14] and biosensing platforms.[15,16] However, despite their widespread use, many of these approaches require elevated operating temperatures or exhibit limited selectivity, which restricts their applicability in real-time monitoring systems.

Chemiresistive sensors offer notable advantages due to their structural simplicity and compatibility with miniaturization. Their operation relies on variations in electrical resistance induced by the adsorption of reducing or oxidizing gases.[17]

[a]*Institute of Combustion Problems, Almaty 050012, Kazakhstan. E-mail: smagulova.gaukhar@gmail.com*
[b]*Al Farabi Kazakh National University, Almaty 050040, Kazakhstan*
[c]*Satbayev University, Almaty 050013, Kazakhstan*
[d]*Abai Kazakh National Pedagogical University, Almaty 050010, Kazakhstan*
[e]*Northwestern Polytechnical University, Xi'an, China*

Sensor performance strongly depends on the morphology of the active layer, the specific surface area, and the electronic structure of the sensing material. To enhance these characteristics, increasing attention has been devoted to 2D materials and hybrid architectures. Graphene and its oxidized derivatives exhibit high adsorption activity,[18] extensive surface area, and tunable surface chemistry, making them highly attractive for the detection of toxic gases, including CO.[19]

Conducting polymers-particularly polyaniline (PANi)-have emerged as promising components for hybrid sensor platforms. PANi provides advantages such as low synthesis cost, tunable conductivity *via* doping, and favorable operational stability.[19–22] In its oxidized, protonated emeraldine salt form, PANi behaves as an electronic conductor, whereas transition to the leuco-emeraldine form results in a substantial decrease in conductivity.[23] This redox-responsive behavior imparts high sensitivity to reducing gases: interaction with CO induces partial deprotonation, charge redistribution, and a corresponding decrease in electrical resistance.

To address the inherent limitations of pristine PANi-including slow relaxation kinetics and a restricted number of active adsorption sites-numerous studies have focused on PANi hybrids with carbon nanomaterials. Reported composites include PANi/GO, PANi/CNTs, and PANi/carbon nanofibers, all demonstrating improved selectivity and significantly enhanced sensing responses.[24,25] Graphene-derived nanocomposites have also been widely explored in electrochemical sensing applications, where rGO-based hybrid electrodes enable efficient charge transfer and high sensitivity toward diverse analytes, including toxic heavy metal ions and small biomolecules, demonstrating the broad applicability of carbon nanostructures in sensing technologies.[26,27] Incorporation of GO promotes the formation of conductive pathways, facilitates charge-carrier transport, and increases the density of adsorption sites. For example, a PANi/GO composite modified with AgCl nanoparticles exhibited a response of ~19.5% at 130 ppm CO with response/recovery times of 50/39 s.[28] Similarly, PANi/GO platforms show lower detection limits and faster dynamic characteristics than pristine PANi.[29] Multicomponent hybrids such as p-PP/CNT/PANi further highlight the critical importance of engineered conductive networks.[30]

PANi/GO composites are particularly promising for room-temperature CO detection. The presence of GO increases the density of active adsorption centers and enables the formation of p–n heterojunctions, which amplify barrier-modulation effects in the presence of reducing gases.[31] These processes result in a pronounced decrease in electrical resistance and accelerated relaxation. A representative PANi/GO sensor demonstrates up to 47% response at 50 ppm CO with response/recovery times of 17/11 s, considerably surpassing pristine PANi.[32]

Despite the fact that PANi/GO composites for the detection of CO and other reducing gases have been widely reported, many previous studies primarily emphasize performance enhancement, while the influence of PANi–GO integration on the electronic structure and chemiresistive behavior of the composite is often discussed only qualitatively.[20,33,34] Furthermore, both graphene oxide and polyaniline are known to exhibit pronounced variability in their physicochemical and electronic properties depending on synthesis conditions, which makes the role of their integration particularly important for achieving reliable sensing performance.

In this work, PANi/GO composites synthesized under well-defined conditions are employed to experimentally elucidate the effect of GO incorporation on charge transport and chemiresistive response. The results demonstrate that integration of GO into the PANi matrix promotes the formation of conductive pathways and leads to a stable and enhanced CO sensing response at room temperature. Accordingly, this study highlights PANi–GO interfacial engineering as a practically viable approach for achieving robust chemiresistive CO sensing at ambient conditions, even in the presence of intrinsic material variability, thereby underscoring the technical relevance of PANi/GO composites for real-world sensing applications.

Materials and methods

The following reagents and materials were used for the synthesis of the nanostructured composites: aniline ($C_6H_5NH_2$), graphene oxide (XFNANO, China), hydrochloric acid (37%, HCl), ammonium persulfate ($(NH_4)_2S_2O_8$), and *N*-methyl-2-pyrrolidone (NMP). The equipment employed included magnetic stirrers (MMS-3000, BioSan; MS-H340-S4, DLAB Scientific), an ultrasonic bath (UC-9120L), spin coater (CY-SP4, Zhengzhou Cy Scientific Instrument Co., Ltd, Henan, China), a single-channel potentiostat/galvanostat (CS350M, Wuhan Corrtest Instruments, China), interdigitated quartz electrodes with 150 fingers, a mass flow controller (MB-2SLPM-D, Alicat, USA), and certified CO gas mixtures (GSO 12331-2023, 500 ppm).

Polymerization of aniline was carried out in an acidic medium. A mixture of 2.5 mL of 1 M HCl and 0.227 mL of aniline was added to a beaker and stirred on a magnetic stirrer in an ice bath (0–5 °C). Separately, 0.57 g of ammonium persulfate ($(NH_4)_2S_2O_8$) was dissolved in 1.82 mL of deionized water and added dropwise to the aniline solution. The reaction proceeded under continuous stirring for 2 h. The precipitate was collected by vacuum filtration, washed with 40 mL of 1 M HCl followed by 10 mL of acetone, and dried at 70 °C for 24 h. A dark green PANi powder was obtained.

The synthesis of the composites was performed *via* oxidative polymerization of aniline in an acidic medium. For this purpose, 0.058 g of GO was first dispersed in ethanol using ultrasonic treatment for 20 min while cooling in an ice bath. The suspension was subsequently dried to remove ethanol completely. The dispersed GO was transferred to a reaction beaker, followed by the addition of 2.5 mL of 1 M HCl and 0.227 mL of aniline. The mixture was stirred on a magnetic stirrer under cooling conditions. The initiator solution-0.57 g of $(NH_4)_2S_2O_8$ dissolved in 1.82 mL of deionized water-was added dropwise. The mass ratio of PANi : GO was maintained at 4 : 1. Polymerization was continued for 2 h. Upon completion, the product was collected by vacuum filtration, washed with 40 mL of 1 M HCl and subsequently with 10 mL of acetone, filtered

again, and dried in an oven at 70 °C for 24 h. The resulting material formed a fine dark green powder.

For gas-sensing tests, the synthesized PANi/GO composites were dispersed in *N*-methyl-2-pyrrolidone (NMP) at a concentration of 20 mg mL^{-1}. The dispersion was ultrasonicated for 30 min in an ice bath to ensure suspension stability. An aliquot of 200 μL of the prepared suspension was deposited onto sensor chips (5 mm × 8 mm × 10 μm) with gold interdigitated electrodes (Au IDE) by spin coating at 3000 rpm for 120 s. After deposition (Fig. S1), the coated chips were vacuum-dried at 70 °C for 24 h to ensure complete solvent removal. For gas-sensing measurements, the potentiostat electrodes were connected to the contact pads of the chip, after which the sensor was placed inside a sealed stainless-steel chamber with a volume of 250 mL. Certified CO mixtures at a concentration of 500 ppm (GSO 12331-2023) were used as test gases. The response characteristics were recorded using the potentiostat software according to the formula:

$$R = \left| \frac{R_{N_2} - R_a}{R_{N_2}} \right| \times 100\%$$

where R_a is the resistance measured in the presence of CO.

Measurements were carried out at a constant voltage of 1 V. Both the response characteristics and the recovery behavior of the sensor were recorded using the potentiostat software. The structure, morphology of the obtained samples were analyzed using a field-emission scanning electron microscope (SEM, Auriga Crossbeam 540, Carl Zeiss, Oberkochen, Germany) at the Core Facilities, Electron Microscopy Laboratory (Nazarbayev University, Astana, Kazakhstan). Surface microstructure was examined with a Leica DM 600 M automated optical microscope (magnification range 150×–1500×) and a Levenhuk MED 30T microscope (40×, 50×). Raman spectra were recorded on an NT-MDT NTegra Spectra spectrometer (KazNU) using a 473 nm excitation laser, with a spectral resolution error of ±0.5 cm^{-1}. X-ray photoelectron spectroscopy (XPS) was carried out on a PHI Quantera II spectrometer (Nanjing University of Science and Technology, China). Gas-sensing properties were investigated using a single-channel potentiostat/galvanostat.

Results and discussion

Scanning electron microscopy (Fig. 1a and b) revealed that the synthesized polyaniline exhibits a predominantly spherical particle morphology. The PANi particles range in size from 200 to 800 nm and tend to aggregate, forming a porous, disordered structure with numerous voids and cavities. Such morphology is typical for PANi obtained *via* oxidative polymerization in an acidic medium and is associated with rapid polymer precipitation and the formation of random interparticle connections. The internal surfaces of the agglomerates appear loose and heterogeneous, indicating a high specific surface area favourable for adsorption processes and interactions with gas molecules. This structural arrangement facilitates more efficient penetration of gas molecules into the material, which is especially important for sensing applications.[35] This type of morphology is often described as sponge-like or quasi-porous and is characteristic of conducting polymers, particularly PANi synthesized using ammonium persulfate as the oxidant.[36,37]

In the case of the PANi/graphene oxide composite (Fig. 1e and f), a more uniform distribution of polymer particles across the graphene layers is observed. The morphology is characterized by strong interfacial interactions between PANi and the graphene structures, while individual agglomerates are still present. This distribution promotes an increased number of contact sites and the formation of an extended conductive network, which positively influences electron transport and can potentially enhance the gas-sensing performance of the material.

XPS was employed to determine the chemical composition and oxidation states of the elements in the obtained materials. The main objectives of this analysis were: (1) to verify the successful synthesis of polyaniline on the GO surface, and (2) to identify the dominant oxidation state of polyaniline, as it governs the intrinsic conductivity and the mechanism of gas–material interaction. It should be noted that XPS is a surface-sensitive technique with an effective probing depth of approximately 5–10 nm. Although it provides precise information on the chemical state of the surface-where gas adsorption processes primarily occur-it does not fully reflect the bulk structure of the material. Nevertheless, for gas-sensing applications, the surface properties are of critical importance.

Raman spectroscopy confirms the structure of the synthesized polyaniline, as shown in Fig. 2a.[38] The spectrum exhibits characteristic peaks at 823 and 871 cm^{-1}, corresponding to the leuco-emeraldine form, as well as intense bands at 1187, 1322, and 1619 cm^{-1}. The band at 1187 cm^{-1} is attributed to C–H deformation vibrations in benzenoid rings, while the peak at 1322 cm^{-1} is associated with polaronic C–N vibrations. The most intense band at 1619 cm^{-1} represents the quinoid C=C structure.[39–41] The strong intensity of polaronic and quinoid vibrations, combined with the pronounced benzenoid ring band, indicates a stably protonated and partially oxidized emeraldine form of polyaniline, which is known to possess good electrical conductivity.[42]

Importantly, the PANi/GO composite retains the characteristic vibrational features of polyaniline. As shown in Fig. 2a, the main bands of PANi-located at ~830 and ~870 cm^{-1} (C–H deformations in benzenoid rings), ~1185 cm^{-1} (C–H), ~1320–1330 cm^{-1} (polaronic C–N vibrations), and ~1600–1620 cm^{-1} (quinoid C=C vibrations)-are fully preserved and coincide with the corresponding bands of pristine PANi.

This indicates that oxidative polymerization proceeds *in situ* on the GO surface, forming a dense polyaniline coating that masks the D and G bands of GO. A similar overlap of the PANi and PANi/GO spectra has been reported by Manivel *et al.*,[43] where it was noted that GO does not alter the conformation of PANi but instead serves as a substrate for its assembly.[44]

The survey spectra (Fig. 2b) confirmed the presence of all expected major elements in the sample: carbon (C 1s), nitrogen (N 1s), and oxygen (O 1s). In the wide-range spectrum of the PANi/GO composite, a weak Cl 2p signal additionally appears, associated with chloride anions that act as counterions in the

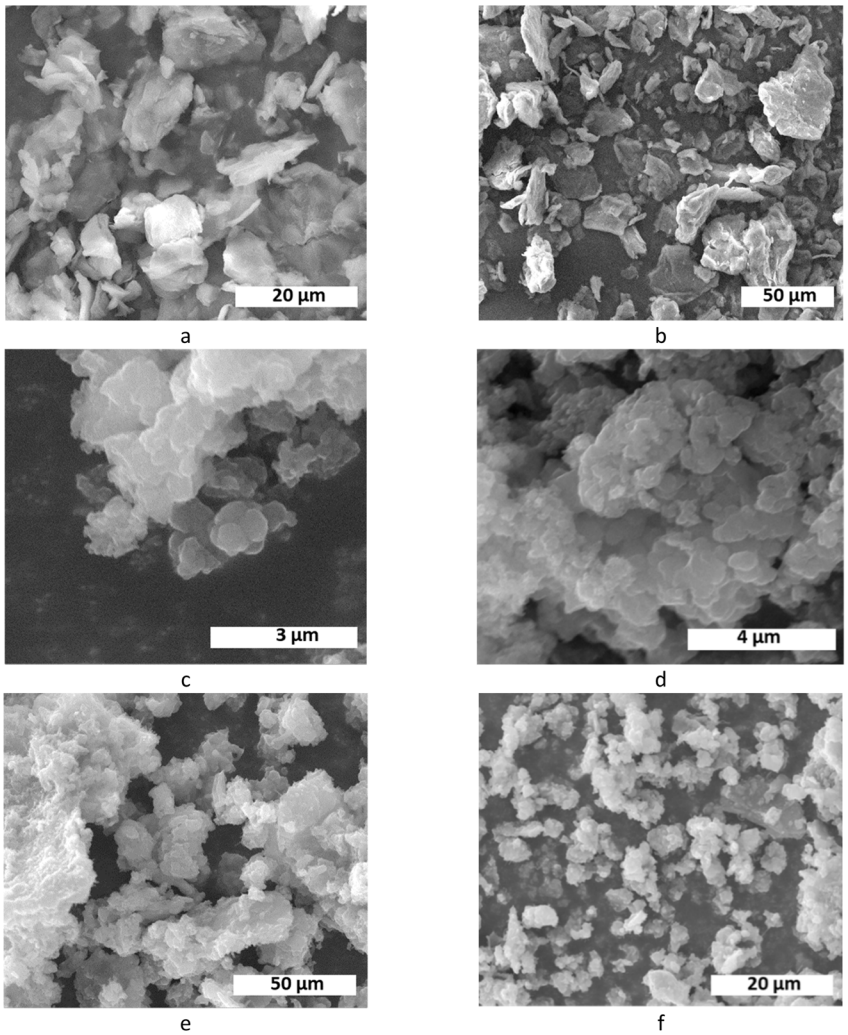

Fig. 1 Morphology: (a and b) GO; (c and d) PANi; (e and f) PANi/GO composite.

emeraldine salt form of PANi synthesized in the HCl/aniline hydrochloride medium. It is well established that during doping of PANi with hydrochloric acid, Cl^- compensates the charge of protonated imine and amine groups (–NH^+–, =N^+H–), leading to an increased fraction of positively charged nitrogen centers and enhanced electrical conductivity.[45]

Detailed analysis of the C 1s spectrum PANi (Fig. 3a) revealed several key C-bonds. The main peak at ~284.5 eV corresponds to C–C/C–H bonds in the aromatic ring, whereas the peak at ~285.5 eV is attributed to C–N/C=N bonds and peak at ~286.5 eV was due to the C–O bonds.[46]

The incorporation of GO, which is rich in oxygen-containing functional groups (–COOH, –OH, –O–), strengthens acid–base and charge–transfer interactions at the PANi/GO interface, stabilizes the polaronic and bipolaronic forms of PANi, and thereby promotes more efficient protonation of the polymer. This behavior is consistent with the reported improvements in electrical conductivity characteristics of PANi/GO composites.[47] The N 1s spectrum of PANi (Fig. 3b) can be deconvoluted into three components centered at 398.3, 399.0, and 400.3 eV, which are assigned to imine (=N–), amine (–NH–) units of the polymer backbone, and protonated imine nitrogen (–NH^+–), respectively.[48,49] An increase in the degree of protonation leads to a more pronounced shoulder in the N 1s spectral envelope.[50] The presence of protonated imine groups also accounts for the detection of chloride anions, which act as counterions to maintain charge neutrality.

Analysis of the PANi/GO composite revealed significant differences in its electronic structure compared to pristine PANi. In the C 1s spectrum (Fig. 3c), the characteristic peaks corresponding to oxygen-containing functional groups of graphene oxide (C–O, C=O), typically observed in the 286–289 eV range,[51] are absent. Instead, the main component appears at an unusually low binding energy of ~283.9 eV. Presumably, during the composite formation process, substantial reduction of graphene oxide occurred, resulting in the removal of most oxygen-containing functional groups and the formation of reduced graphene oxide (rGO). Similar findings were reported in work,[52] where a PANi/rGO composite was obtained *via* a one-step reduction of GO during the oxidative polymerization process.

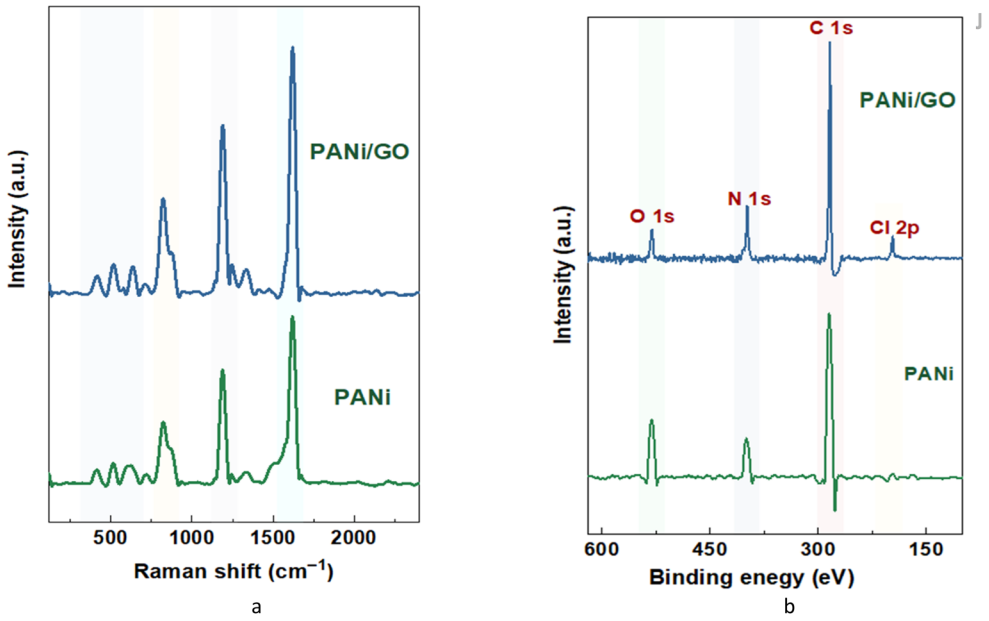

Fig. 2 Raman spectrum (a) and XPS survey scan (b).

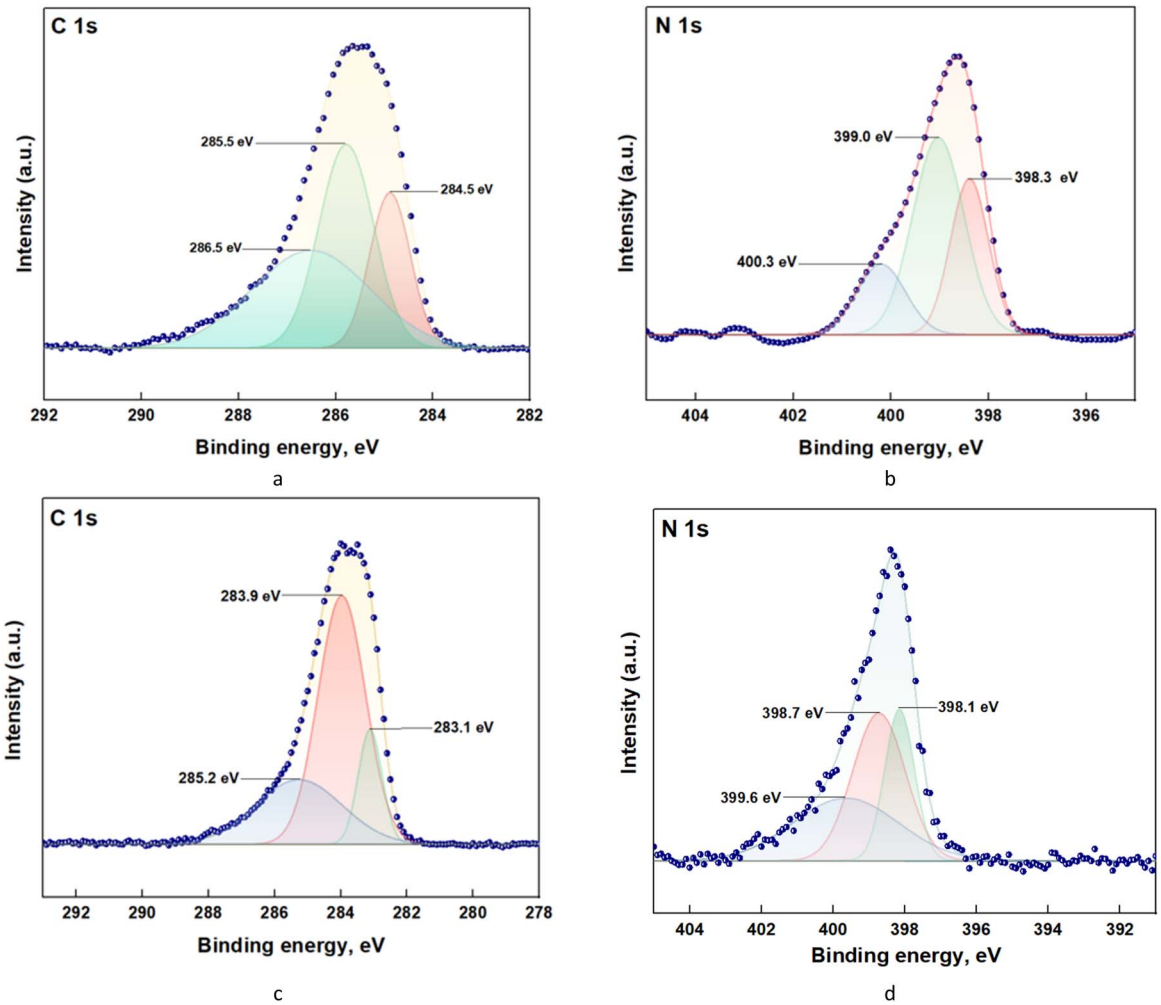

Fig. 3 Deconvolution of the XPS C 1s and N 1s peaks for the synthesized samples: (a and b) PANi; (c and d) PANi/graphene oxide composite.

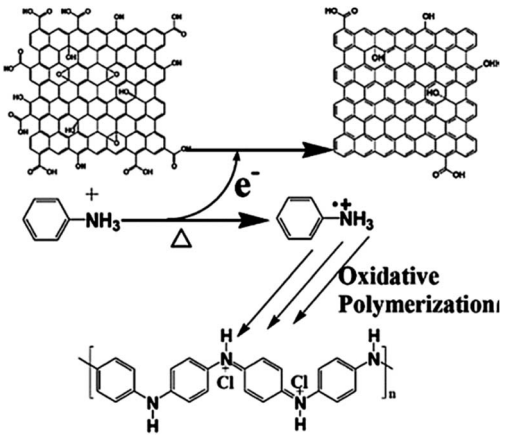

Fig. 4 Schematic illustration of the formation of the PANi/rGO composite *via* oxidative polymerization of aniline on the surface of GO.[52]

The C 1s core-level spectrum of the PANi/GO composite can be deconvoluted into three main components with binding energies at approximately 283.9, 285.2, and 283.1 eV, which can be attributed to sp^2-hybridized carbon (C=C and C=O bonds) and sp^3-hybridized carbon (C–C and C–H bonds).[53] In contrast to the expected shift to higher binding energies due to hydrogen bonding with oxygen-containing groups, the main nitrogen peak shifts to lower binding energy (~398.7 eV) relative to pristine PANi (~399.0 eV) (Fig. 3d). Such a shift indicates increased electron density along the polymer chain and is presumably the result of electron transfer from the reduced sp^2-rich regions of rGO to the PANi backbone.

Therefore, the XPS data suggest that under the employed synthesis conditions, graphene oxide does not act merely as an inert substrate with "anchoring groups", but instead functions as a reducing agent, converting into rGO and forming a composite with strong electronic coupling to PANi (Fig. 4). Charge transfer and the formation of highly conductive rGO domains within the PANi matrix likely contribute to the enhanced sensing performance of the composite.

Thus, the combined XPS and Raman analyses confirm the successful formation of conducting polyaniline in its half-oxidized and protonated emeraldine form. The conductivity of polyaniline is governed by two key mechanisms: charge delocalization along the polymer chains and tunneling transitions between adjacent chains.[54,55]

As shown in Fig. 5a, both PANi and the PANi/GO composite exhibit a gas-sensitive response upon exposure to CO. The PANi sensing layer forms a conductive channel between the electrodes, enabling detection of resistance changes upon interaction with the gas phase. Fig. 5 presents the response of the PANi-based sensor (Fig. 5a), the PANi/GO sensor (Fig. 5b), and the cycling stability of the PANi/GO composite during repeated CO detection cycles followed by recovery in a nitrogen atmosphere.

The sensing response of pristine PANi toward CO reached 9.72%, with a response time of 168 s and a recovery time of 16.78 min (Fig. 5a). In contrast, the PANi/graphene oxide

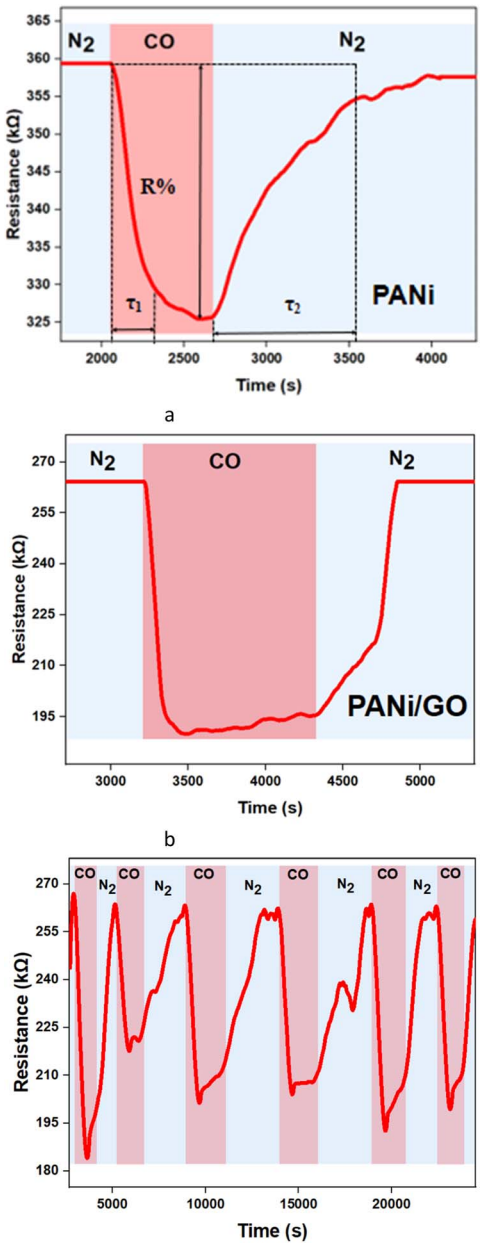

Fig. 5 Gas-sensing performance of (a) PANi and (b) PANi/GO; (c) cyclic stability of the PANi/GO sensor.

composite demonstrated a significantly enhanced response of 31.48%, accompanied by an increase in response time to 360 s and a reduction in recovery time to 9.95 min. The gas-sensing characteristics of the composite were additionally examined toward methane, regarded as a potential interfering species. The PANi/GO composite showed a response of approximately 5.88% to CH_4, confirming its pronounced selectivity toward CO over CH_4 (Fig. S2).

PANi and GO are p-type semiconductors; the conductivity of PANi is attributed to its hole-transport properties.[56] The electrical conductivity of acid-doped PANi results from structural modifications, while the number of electrons in the conjugated polymer backbone remains unchanged. The nitrogen atoms of

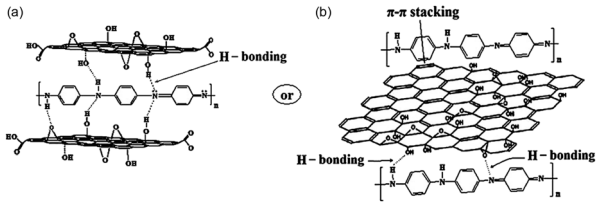

Fig. 6 Schematic illustration of the interaction between graphene oxide sheets and polyaniline chains.[58]

the imine groups become protonated, forming positively charged species that induce structural distortion within the polymer chain. The charges are primarily localized in bipolaron centers, and internal redox processes convert bipolaron charges into a polaron lattice structure, in which polarons are delocalized along the polymer chains. The doping process enables charge transport through the π-electron system.[57]

The incorporation of GO into the PANi/GO composite enhances sensor sensitivity due to the formation of a three-dimensional porous nanostructure with increased specific surface area, a higher density of vacancies and defects, and a greater number of active adsorption sites for CO. In addition, π–π interactions between GO sheets and PANi chains contribute to improved charge transfer.[29]

As reported in work,[58] during polymerization, aniline molecules can adsorb onto the surface and within the interlayer spacing of GO and subsequently polymerize in the presence of an oxidant, forming the PANi/GO composite. The possible formation of hydrogen bonds between GO and PANi in the composite is schematically illustrated in Fig. 6a. Hydroxyl (–OH), carboxyl (–COOH), and epoxy groups present on the surface and within the pores of GO facilitate hydrogen bonding with the amine and imine nitrogen atoms of the benzenoid and quinoid units of the polymer chain. Furthermore, π–π stacking interactions between the polymer backbone and GO sheets are also expected (Fig. 6b).

CO belongs to the group of reducing gases. Upon exposure to CO, the response of a PANi-based sensor is manifested as a decrease in the electrical resistance of the sensing layer due to partial charge transfer between the –NH groups in the polymer and the carbocationic species of CO.[59] As demonstrated in work,[60] the self-diffusion coefficient for the PANi/rGO composite is 5.83×10^{-10} m^2 s^{-1}, indicating the possibility of CO molecule diffusion within the PANi/graphene structure. The transferred charge propagates along the polymer chain, resulting in an increase in the electrical conductivity of the layer.

The schematic representation of the CO sensing mechanism on PANi is shown in Fig. 7. The observed enhancement in electrical conductivity can be attributed to an increase in the concentration of charge carriers, as described by the relation $\Delta\sigma = e\mu\Delta n$, where e represents the elementary charge, μ denotes the charge carrier mobility, and Δn corresponds to the increase in charge carrier density.[61]

PANi interacts with carbon-based nanomaterials containing sp^2 bonds through π–π interactions, which facilitate charge transfer processes and thereby enhance charge carrier

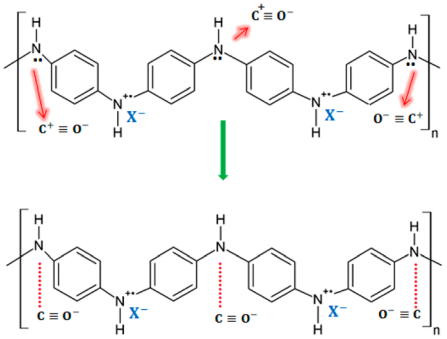

Fig. 7 Mechanism of interaction between PANi and CO molecules.[62]

delocalization. As a result, rGO–PANi composites exhibit improved performance as electrically active sensing layers.[64]

However, the increase in the sensor response of the PANi/GO composite is accompanied by a deterioration in response time, which rises from 168 s for pristine PANi to 360 s for PANi/GO. As shown previously, the active sites of the PANi/GO gas-sensitive composite are the amine groups within the PANi structure. A relatively small CO molecule can directly reach an active site of the sensing material only with a certain probability. In most interaction events, after overcoming the adsorption barrier, the CO molecule must diffuse to reach the active gas-sensitive sites of the sensor, which slows down the response and leads to an increase in response time.[65]

Gas sensing should be considered as a coupled diffusion–reaction process, where the sensor response is governed not only by the chemical composition of the material but also by its structural organization.[66,67] The presence of phase boundaries, porosity, and structural defects significantly affects gas transport pathways and surface reaction kinetics, thereby influencing both the sensor response and, in particular, the response and recovery times. Consequently, gas-sensing performance is strongly controlled by the microstructural and textural features of the sensing layer, which determine the accessibility of active sites and the dynamics of adsorption–desorption processes.

An additional contribution to the increased response time may arise from the presence of phase boundaries between PANi and GO, as well as grain boundaries. Moreover, the response time depends on the balance between adsorption and desorption processes occurring at the surface of the gas sensor. Overall, investigations of interaction mechanisms at the atomic level are of fundamental importance for a deeper understanding of sensing processes and for the atomic-scale tuning of structure to achieve optimal sensitivity and selectivity.

Thus, the incorporation of GO leads to nearly a threefold increase in sensor response, although it is accompanied by a longer recovery time, which is consistent with literature reports indicating a higher density of active sites on the surface of composite materials.[68] As shown in Table 1, gas exposure even at room temperature leads to a noticeable increase in resistance; however, the sensitivity and kinetics of pristine PANi depend strongly on both concentration and film morphology.

Table 1 Summary of CO sensing performance of PANi-based and PANi/GO composite sensors at room temperature

Material	Response, %	Response/recovery time, s	Operating temperature, °C	Analyte	Concentration, ppm	Ref.
PANi	27	180/200	RT	CO	6000	69
PANi	—	66/330	RT	CO	1000	63
PANi	0.26	45/121	RT	CO	100	72
PANi	9.4	N/A	RT	CO	1000	68
PANi	9.72	168/16.78 min	RT	CO	500	This work
PANi/GO	31.48	360/9.95 min	RT	CO	500	This work

At 6000 ppm CO, the response reaches 27%,[69] whereas at 1 ppm it decreases to 18%.[70] The highest reported response of 37% at 2.5 ppb with a response time of approximately 20 s was obtained for a thin-film system with a high degree of protonation, highlighting the crucial role of the concentration of h^+ charge carriers in signal formation.[71]

Overall, studies demonstrate the promising potential of developing sensitive and selective PANi-based gas sensors, particularly those modified with GO, which may find practical application for CO detection in environmental monitoring and industrial process control and safety.[73]

Conclusions

The present study demonstrates that chemiresistive sensing materials based on polyaniline deposited onto graphene oxide exhibit strong potential for room-temperature detection of carbon monoxide. Pristine PANi displayed a typical p-type sensing behavior with a CO response of ~9.7% and a response time of ~168 s. Incorporation of graphene oxide resulted in a significant improvement in sensing performance: the PANi/GO composite exhibited an enhanced response of ~31.5%, indicating a pronounced synergistic interaction between the conducting polymer and the carbon framework.

Electron microscopy confirmed that the PANi/GO composite retains a highly porous and morphologically complex structure, providing a large number of accessible adsorption sites for CO molecules and facilitating gas diffusion within the sensing layer. Raman spectroscopy and XPS analysis revealed partial reduction of the initial graphene oxide during composite formation, as evidenced by C 1s peak deconvolution showing contributions from both sp^2- and sp^3-hybridized carbon. Such structural evolution promotes improved electrical conductivity and interfacial charge transfer within the composite.

The sensing mechanism is attributed to the interaction of CO molecules with imine groups of the PANi/GO composite, leading to additional protonation of the polymer chains and a decrease in electrical resistance. Simultaneously, π–π interactions between polyaniline chains and sp^2 domains of graphene oxide facilitate charge transfer processes and enhance carrier delocalization throughout the hybrid structure. These combined effects result in a higher sensor response and improved signal stability.

Overall, the results highlight several key design principles for high-performance PANi-based gas sensors operating at room temperature: (i) precise control over the protonation level and redox state of polyaniline to achieve optimal conductivity and sensitivity; and (ii) integration of carbon nanostructures such as graphene oxide as a conductive and structurally adaptive framework that effectively modulates the electronic structure of the composite, promotes charge delocalization within the hybrid sensing layer. The obtained findings confirm the promising potential of PANi/GO composites as efficient room-temperature sensing materials for carbon monoxide detection and provide guidance for the rational design of next-generation polymer–carbon hybrid gas sensors.

Author contributions

Imash Aigerim and Smagulova Gaukhar conceived and designed the study. Imash Aigerim performed the experimental work, data curation, validation, and preparation of the original manuscript draft. Kazhdanbekov Ramazan contributed to data processing and software-related tasks, while Kaidar Bayan assisted with formal analysis. Efremov Vladimir supported the experimental investigation. Mansurov Zulkhair provided scientific oversight and advisory input. Smagulova Gaukhar and Imash Aigerim contributed to the writing, review, and editing of the final manuscript.

Conflicts of interest

There are no conflicts to declare.

Data availability

All data supporting the findings of this study are available within the article and its supplementary information (SI).

Supplementary information: optical micrographs of pristine and coated IDE samples before and after sensing-layer deposition (Fig. S1) and the room-temperature gas-sensing performance of the PANi/GO composite toward CH_4 (Fig. S2). See DOI: https://doi.org/10.1039/d5ra09053a.

Acknowledgements

This work was partly supported by the postdoctoral program of Abai Kazakh National Pedagogical University (order no. 05-04/549, June 18, 2025).

References

1 S. Luo, R. Tu, W. Liu, J. Li, J. Li, K. Wang, *et al.*, Adsorption of gas molecules (C_2H_6, CO, H_2S, CH_2O, CH4, and CO_2) on GeC monolayer: A first-principles study, *Comput. Theor. Chem.*, 2025, **1249**, 115263, DOI: 10.1016/j.comptc.2025.115263.

2 A. Fiehn, J. Kostinek, M. Eckl, T. Klausner, M. Gałkowski, J. Chen, *et al.*, Estimating CH_4 , CO_2 and CO emissions from coal mining and industrial activities in the Upper Silesian Coal Basin using an aircraft-based mass balance approach, *Atmos. Chem. Phys.*, 2020, **20**(21), 12675–12695, DOI: 10.5194/acp-20-12675-2020.

3 D. Gilfillan and G. Marland, CDIAC-FF: global and national CO_2 emissions from fossil fuel combustion and cement manufacture: 1751–2017, *Earth Syst. Sci. Data*, 2021, **13**(4), 1667–1680, DOI: 10.5194/essd-13-1667-2021.

4 M. M. Villar-Ramos, I. Hernández-Pérez, K. M. Aguilar-Castro, I. Zavala-Guillén, E. V. Macias-Melo, I. Hernández-López, *et al.*, A Review of Thermally Activated Building Systems (TABS) as an Alternative for Improving the Indoor Environment of Buildings, *Energies*, 2022, **15**(17), 6179, DOI: 10.3390/en15176179.

5 J. Yu, J. Lee, Y. Cho, J. Oh, H. Kang, T. H. Lim, *et al.*, Correlation between Carboxyhemoglobin Levels Measured by Blood Gas Analysis and by Multiwave Pulse Oximetry, *J. Pers. Med.*, 2024, **14**(2), 168, DOI: 10.3390/jpm14020168.

6 H. Wu, G. Lin, H. Xie, S. Li, H. He and T. Jiang, Adsorption and sensing properties of Janus MoSTe materials for characteristic gases (CO, C_2H_2, C_2H_4, CH_4) in power transformers: A DFT study, *Int. J. Hydrogen Energy*, 2025, **102**, 1253–1266, DOI: 10.1016/j.ijhydene.2025.01.124.

7 Y. Mao, N. Li, H. Chen and D. Ding, The sensing properties of asphyxiating gas molecules (CH_4, CO and H_2S) adsorption on GaP3 monolayer: A first principle study, *Mater. Today Commun.*, 2024, **39**, 108649, DOI: 10.1016/j.mtcomm.2024.108649.

8 World Health Organization, Ambient (outdoor) air quality and health, available from: https://www.who.int/news-room/fact-sheets/detail/ambient-(outdoor)-air-quality-and-health, accessed November 23, 2025.

9 A. Kalinichenko, A. Sackmann, B. Junker, U. Weimar and N. Bârsan, Novel method for monitoring residual hexane in refined oils using semiconducting metal oxide-based gas sensors, *Sens. Actuators, B*, 2025, **434**, 137616, DOI: 10.1016/j.snb.2025.137616.

10 A. Gupta, A. G. Ravelo-García and F. M. Dias, Availability and performance of face based non-contact methods for heart rate and oxygen saturation estimations: A systematic review, *Comput. Methods Progr. Biomed.*, 2022, **219**, 106771, DOI: 10.1016/j.cmpb.2022.106771.

11 A. Hosoya, S. Tamura and N. Imanaka, A New Catalytic Combustion-type Carbon Monoxide Gas Sensor Employing Precious Metal-free CO Oxidizing Catalyst, *ISIJ Int.*, 2015, **55**(8), 1699–1701, DOI: 10.2355/isijinternational.ISIJINT-2015-134.

12 F. Li, Y. Akiyama, X. Wan, S. Okamoto and Y. Yamada, Measurement of Shear Strain Field in a Soft Material Using a Sensor System Consisting of Distributed Piezoelectric Polymer Film, *Sensors*, 2020, **20**(12), 3484, DOI: 10.3390/s20123484.

13 Y. Wang, Q. Xiang, Q. Zhou and N. Liao, First-principles prediction of Ni-MoO3 as selective and sensitive sensor for detecting CO over CH4, H2, H2O, NH3, H2S gases, *Phys. Lett. A*, 2024, **526**, 129981, DOI: 10.1016/j.physleta.2024.129981.

14 S. G. Manjushree, S. Ashoka and P. S. Adarakatti, A brief review on basic principles of electrochemistry and electrochemical sensing devices, in *Real-Time Applications of Advanced Electrochemical Sensing Devices*, ed Manjunatha J. G., IOP Publishing, 2024, pp. 111–120, DOI: 10.1088/978-0-7503-5377-9ch1, available from: https://iopscience.iop.org/book/edit/978-0-7503-5377-9/chapter/bk978-0-7503-5377-9ch1.

15 P. S. Adarakatti and C. E. Banks, Advances in electrochemical sensing and catalysis: bridging fundamentals and applications, in *Electrochemistry*, ed. Banks C. E., Royal Society of Chemistry, 2025, pp. 85–120, DOI: 10.1039/9781837070244-00085, available from: https://books.rsc.org/books/book/2476/chapter/8746971/Advances-in-electrochemical-sensing-and-catalysis.

16 B. P. Suma and P. S. Adarakatti, Brief Overview of Different Biosensors: Properties, Applications, and Their Role in Chemistry, in *Biosensing Technology for Human Health*, ed. Manjunatha J. G., Royal Society of Chemistry, 2024, DOI: 10.1039/9781837676323-00001, pp. 1–32, Available from: https://books.rsc.org/books/book/2256/chapter/8246363/Brief-Overview-of-Different-Biosensors-Properties.

17 M. Eising, C. O'Callaghan, C. Eduardo Cava, A. Schmidt, A. J. Gorgatti Zarbin, M. S. Ferreira, *et al.*, The role of carbon nanotubes on the sensitivity of composites with polyaniline for ammonia sensors, *Carbon Trends*, 2021, **3**, 100026, DOI: 10.1016/j.cartre.2021.100026.

18 L. BT, Synthesis of Nanomaterials in a Coaxial Flame, *Eurasian Chem.-Technol. J.*, 2020, **22**(3), 177–185, DOI: 10.18321/ectj977.

19 D. Panda, A. Nandi, S. K. Datta, H. Saha and S. Majumdar, Selective detection of carbon monoxide (CO) gas by reduced graphene oxide (rGO) at room temperature, *RSC Adv.*, 2016, **6**(53), 47337–47348, DOI: 10.1039/C6RA06058G.

20 J. Kroutil, A. Laposa, V. Povolny, L. Klimsa and M. Husak, Gas Sensor with Different Morphology of PANI Layer, *Sensors*, 2023, **23**(3), 1106, DOI: 10.3390/s23031106.

21 A. H. Majeed, L. A. Mohammed, O. G. Hammoodi, S. Sehgal, M. A. Alheety, K. K. Saxena, *et al.*, A Review on Polyaniline: Synthesis, Properties, Nanocomposites, and Electrochemical Applications, *Int. J. Polym. Sci.*, 2022, **2022**, 1–19, DOI: 10.1155/2022/9047554.

22 N. Sharma, A. Singh, N. Kumar, A. Tiwari, M. Lal and S. Arya, A review on polyaniline and its composites: from synthesis to properties and progressive applications, *J. Mater. Sci.*, 2024, **59**(15), 6206–6244, DOI: 10.1007/s10853-024-09562-z.

23 C. M. Masemola, N. Moloto, Z. Tetana, L. Z. Linganiso, T. E. Motaung and E. C. Linganiso-Dziike, Advances in Polyaniline-Based Composites for Room-Temperature Chemiresistor Gas Sensors, *Processes*, 2025, **13**(2), 401, DOI: 10.3390/pr13020401.

24 D. Lv, W. Shen, W. Chen, Y. Wang, R. Tan, M. Zhao, *et al.*, One-step preparation of flexible citric acid-doped polyaniline gas sensor for ppb-level ammonia detection at room temperature, *Sens. Actuators, A*, 2023, **350**, 114120, DOI: 10.1016/j.sna.2022.114120.

25 B. Li, Y. Li and P. Ma, Synthesis of different inorganic acids doped polyaniline materials and behavior of enhancing NH3 gas sensing properties, *Org. Electron.*, 2023, **114**, 106749, DOI: 10.1016/j.orgel.2023.106749.

26 R. B. Manami, M. B. Megalamani, R. G. Kalkhambkar, P. S. Adarakatti, S. T. Nandibewoor, K. Narasimharao, *et al.*, Advancement in highly selective electrochemical sensing of Pb (II) using CuWO4/RGO nanocomposite modified electrode, *J. Mater. Sci.: Mater. Electron.*, 2025, **36**(36), 2268, DOI: 10.1007/s10854-025-16316-3.

27 R. B. Manami, M. B. Megalamani, R. G. Kalkhambkar, S. T. Nandibewoor, P. S. Adarakatti, K. Narasimharao, *et al.*, High-performance detection of tryptophan using a $NiWO_4$/RGO nanohybrid modified electrode in environmental applications, *Ionics*, 2026, **17**, 1–21, DOI: 10.1007/s11581-025-06879-w.

28 H. Y. Mohammed, M. S. Birare, M. A. Farea, M. N. Murshed, M. E. El Sayed, A. Samir, *et al.*, Accelerated kinetics for room temperature carbon monoxide sensing enabled by silver chloride-modified protonated polyaniline/graphene oxide, *Appl. Phys. A*, 2024, **130**(1), 39, DOI: 10.1007/s00339-023-07189-6.

29 H. Y. Mohammed, M. A. Farea, P. W. Sayyad, N. N. Ingle, T. Al-Gahouari, M. M. Mahadik, *et al.*, Selective and sensitive chemiresistive sensors based on polyaniline/graphene oxide nanocomposite: A cost-effective approach, *J. Sci. Adv. Mater. Devices*, 2022, **7**(1), 100391, DOI: 10.1016/j.jsamd.2021.08.004.

30 S. M. Aalam, A. Farooq, M. Sarvar, M. N. Bhat, M. Tomar, M. M. H. Raza, *et al.*, To study the performance of polyaniline-based copper and carbon-nanotube (PANI@Cu@CNT) nanocomposite for harmful NH3 gas sensing, *Sci. Rep.*, 2025, **15**(1), 26886, DOI: 10.1038/s41598-025-01055-6.

31 M. N. Norizan, N. Abdullah, N. A. Halim, S. Z. N. Demon and I. S. Mohamad, Heterojunctions of rGO/Metal Oxide Nanocomposites as Promising Gas-Sensing Materials—A Review, *Nanomaterials*, 2022, **12**(13), 2278, DOI: 10.3390/nano12132278.

32 A. Arularasan, K. Venkataramani, B. Venkatachalam Rajarajan, S. Jeyaraman, A. Kumar and R. Kannan, Simulation performance of inkjet-printed polyaniline–graphene oxide nanocomposite based gas sensor, *Microsyst. Technol.*, 2024, **30**(11), 1463–1476, DOI: 10.1007/s00542-024-05661-8.

33 Y. Yan, G. Yang, J. L. Xu, M. Zhang, C. C. Kuo and S. D. Wang, Conducting polymer-inorganic nanocomposite-based gas sensors: a review, *Sci. Technol. Adv. Mater.*, 2020, **21**(1), 768–786, DOI: 10.1080/14686996.2020.1820845.

34 J. Wen, S. Wang, J. Feng, J. Ma, H. Zhang, P. Wu, *et al.*, Recent progress in polyaniline-based chemiresistive flexible gas sensors: design, nanostructures, and composite materials, *J. Mater. Chem. A*, 2024, **12**(11), 6190–6210, DOI: 10.1039/D3TA07687C.

35 T. N. A. B. T. A. Mutalib, S. J. Tan, K. L. Foo, Y. M. Liew, C. Y. Heah and M. M. A. B. Abdullah, Properties of polyaniline/graphene oxide (PANI/GO) composites: effect of GO loading, *Polym. Bull.*, 2021, **78**(9), 4835–4847, DOI: 10.1007/s00289-020-03334-w.

36 Q. Sun, M. C. Park and Y. Deng, Studies on one-dimensional polyaniline (PANI) nanostructures and the morphological evolution, *Mater. Chem. Phys.*, 2008, **110**(2–3), 276–279, DOI: 10.1016/j.matchemphys.2008.02.014.

37 J. Wang, J. Wang, Z. Yang, Z. Wang, F. Zhang and S. Wang, A novel strategy for the synthesis of polyaniline nanostructures with controlled morphology, *React. Funct. Polym.*, 2008, **68**(10), 1435–1440, DOI: 10.1016/j.reactfunctpolym.2008.07.002.

38 M. C. Bernard and A. Hugot-Le Goff, Raman spectroscopy for the study of polyaniline, *Synth. Met.*, 1997, **85**(1–3), 1145–1146, DOI: 10.1016/S0379-6779(97)80187-7.

39 M. C. Bernard and A. Hugot-Le Goff, Quantitative characterization of polyaniline films using Raman spectroscopy, *Electrochim. Acta*, 2006, **52**(2), 595–603, DOI: 10.1016/j.electacta.2006.05.039.

40 A. Rakić, M. Vukomanović and G. Ćirić-Marjanović, Formation of nanostructured polyaniline by dopant-free oxidation of aniline in a water/isopropanol mixture, *Chem. Pap.*, 2014, **68**(3), 372–383, DOI: 10.2478/s11696-013-0453-2.

41 J. Tokarský, M. Maixner, P. Peikertová, L. Kulhánková and J. V. Burda, The IR and Raman spectra of polyaniline adsorbed on the glass surface; comparison of experimental, empirical force field, and quantum chemical results, *Eur. Polym. J.*, 2014, **57**, 47–57, DOI: 10.1016/j.eurpolymj.2014.04.023.

42 R. Mažeikienė, G. Niaura and A. Malinauskas, A comparative multiwavelength Raman spectroelectrochemical study of polyaniline: a review, *J. Solid State Electrochem.*, 2019, **23**(6), 1631–1640, DOI: 10.1007/s10008-019-04289-3.

43 P. Manivel, M. Dhakshnamoorthy, A. Balamurugan, N. Ponpandian, D. Mangalaraj and C. Viswanathan, Conducting polyaniline-graphene oxide fibrous nanocomposites: preparation, characterization and simultaneous electrochemical detection of ascorbic acid, dopamine and uric acid, *RSC Adv.*, 2013, **3**(34), 14428, DOI: 10.1039/c3ra42322k.

44 A. Balboa-Palomino, U. Páramo-García, J. A. Melo-Banda, J. Y. Verde-Gómez and N. V. Gallardo-Rivas, Effect of Graphene Oxide Addition on the Properties of Electrochemically Synthesized Polyaniline–Graphene Oxide Films, *Polymers*, 2024, **16**(12), 1677, DOI: 10.3390/polym16121677.

45 H. R. Tantawy, B. A. F. Kengne, D. N. McIlroy, T. Nguyen, D. Heo, Y. Qiang, *et al.*, X-ray photoelectron spectroscopy

analysis for the chemical impact of solvent addition rate on electromagnetic shielding effectiveness of HCl-doped polyaniline nanopowders, *J. Appl. Phys.*, 2015, **118**(17), 175501, DOI: 10.1063/1.4934851.

46 B. Sreedhar, M. Sairam, D. K. Chattopadhyay, P. P. Mitra and D. V. M. Rao, Thermal and XPS studies on polyaniline salts prepared by inverted emulsion polymerization, *J. Appl. Polym. Sci.*, 2006, **101**(1), 499–508, DOI: 10.1002/app.23301.

47 Y. Tang, X. Hu, D. Liu, D. Guo and J. Zhang, Effect of Microwave Treatment of Graphite on the Electrical Conductivity and Electrochemical Properties of Polyaniline/Graphene Oxide Composites, *Polymers*, 2016, **8**(11), 399, DOI: 10.3390/polym8110399.

48 S. Golczak, A. Kanciurzewska, M. Fahlman, K. Langer and J. Langer, Comparative XPS surface study of polyaniline thin films, *Solid State Ionics*, 2008, **179**(39), 2234–2239, DOI: 10.1016/j.ssi.2008.08.004.

49 B. J. Waghmode, S. H. Patil, M. M. Jahagirdar, V. S. Patil, R. P. Waichal, D. D. Malkhede, *et al.*, Studies on morphology of polyaniline films formed at liquid–liquid and solid–liquid interfaces at 25 and 5 °C, respectively, and effect of doping, *Colloid Polym. Sci.*, 2014, **292**(5), 1079–1089, DOI: 10.1007/s00396-013-3150-3.

50 K. L. Tan, B. T. G. Tan, E. T. Kang and K. G. Neoh, X-ray photoelectron spectroscopy studies of the chemical structure of polyaniline, *Phys. Rev. B: Condens. Matter Mater. Phys.*, 1989, **39**(11), 8070–8073, DOI: 10.1103/PhysRevB.39.8070.

51 R. Al-Gaashani, A. Najjar, Y. Zakaria, S. Mansour and M. A. Atieh, XPS and structural studies of high quality graphene oxide and reduced graphene oxide prepared by different chemical oxidation methods, *Ceram. Int.*, 2019, **45**(11), 14439–14448, DOI: 10.1016/j.ceramint.2019.04.165.

52 L. Q. Xu, Y. L. Liu, K. Neoh, E. Kang and G. D. Fu, Reduction of Graphene Oxide by Aniline with Its Concomitant Oxidative Polymerization, *Macromol. Rapid Commun.*, 2011, **32**(8), 684–688, DOI: 10.1002/marc.201000765.

53 K. F. Qasim, A. Al-Yamany, S. K. Mohamed and E. M. Saad, Structural, Dielectric, and Electrochemical Behaviour for Polyaniline, Graphene Oxide and their Composite's Mechanism Towards Dichromate Sensing, *J. Inorg. Organomet. Polym.*, 2025, **35**(12), 10099–10109, DOI: 10.1007/s10904-025-03884-4.

54 A. A. Jabor, DrA. M. Farhan, DrA. H. K. Elttayef and A. A. Jabor, Preparation Poly 4-Bromoaniline Thin Films by Electro Deposition Technique for Hydrogen gas sensor, *J. Phys.: Conf. Ser.*, 2018, **1032**, 012063, DOI: 10.1088/1742-6596/1032/1/012063.

55 S. Z. Mohammadabadi and A. R. Zanganeh, Electrochemically Generated Recognition Sites in Self-doped Polyaniline Modified Electrodes for Voltammetric and Potentiometric Determination of Copper(II) Ion, *Electroanalysis*, 2018, **30**(3), 415–425, DOI: 10.1002/elan.201700496.

56 G. Gaikwad, P. Patil, D. Patil and J. Naik, Synthesis and evaluation of gas sensing properties of PANI based graphene oxide nanocomposites, *Mater. Sci. Eng., B*, 2017, **218**, 14–22, DOI: 10.1016/j.mseb.2017.01.008.

57 D. C. Johnson, J. A. Samol and A. O. Sezer, Polyaniline–Graphene Oxide–Titanium Dioxide-Based Ternary Composite for Sensing Applications of Ammonia and Carbon Monoxide, *Nano Select*, 2026, **7**(1), e70061, DOI: 10.1002/nano.70061.

58 S. Konwer, A. K. Guha and S. K. Dolui, Graphene oxide-filled conducting polyaniline composites as methanol-sensing materials, *J. Mater. Sci.*, 2013, **48**(4), 1729–1739, DOI: 10.1007/s10853-012-6931-z.

59 N. Densakulprasert, L. Wannatong, D. Chotpattananont, P. Hiamtup, A. Sirivat and J. Schwank, Electrical conductivity of polyaniline/zeolite composites and synergetic interaction with CO, *Mater. Sci. Eng., B*, 2005, **117**(3), 276–282, DOI: 10.1016/j.mseb.2004.12.006.

60 Z. Guo, N. Liao, M. Zhang and W. Xue, Theoretical approach to evaluate graphene/PANI composite as highly selective ammonia sensor, *Appl. Surf. Sci.*, 2018, **453**, 336–340, DOI: 10.1016/j.apsusc.2018.05.108.

61 S. Watcharaphalakorn, L. Ruangchuay, D. Chotpattananont, A. Sirivat and J. Schwank, Polyaniline/polyimide blends as gas sensors and electrical conductivity response to CO–N2 mixtures, *Polym. Int.*, 2005, **54**(8), 1126–1133, DOI: 10.1002/pi.1815.

62 M. Savin, C. M. Mihailescu, C. Moldovan, A. Grigoroiu, I. Ion and A. C. Ion, Resistive Chemosensors for the Detection of CO Based on Conducting Polymers and Carbon Nanocomposites: A Review, *Molecules*, 2022, **27**(3), 821, DOI: 10.3390/molecules27030821.

63 Y. Wanna, N. Srisukhumbowornchai, A. Tuantranont, A. Wisitsoraat, N. Thavarungkul and P. Singjai, The Effect of Carbon Nanotube Dispersion on CO Gas Sensing Characteristics of Polyaniline Gas Sensor, *J. Nanosci. Nanotechnol.*, 2006, **6**(12), 3893–3896, DOI: 10.1166/jnn.2006.675.

64 F. S. Hadano, A. E. X. Gavim, J. C. Stefanelo, S. L. Gusso, A. G. Macedo, P. C. Rodrigues, *et al.*, NH3 Sensor Based on rGO-PANI Composite with Improved Sensitivity, *Sensors*, 2021, **21**(15), 4947, DOI: 10.3390/s21154947.

65 H. F. Zhang, B. Y. Ning, T. C. Weng, D. P. Wu and X. J. Ning, What retards the response of graphene based gaseous sensor, *Sens. Actuators, A*, 2019, **295**, 188–192, DOI: 10.1016/j.sna.2019.05.044.

66 N. Matsunaga, G. Sakai, K. Shimanoe and N. Yamazoe, Diffusion equation-based study of thin film semiconductor gas sensor-response transient, *Sens. Actuators, B*, 2002, **83**(1–3), 216–221, DOI: 10.1016/S0925-4005(01)01043-7.

67 N. Matsunaga, G. Sakai, K. Shimanoe and N. Yamazoe, Formulation of gas diffusion dynamics for thin film semiconductor gas sensor based on simple reaction–diffusion equation, *Sens. Actuators, B*, 2003, **96**(1–2), 226–233, DOI: 10.1016/S0925-4005(03)00529-X.

68 A. Roy, A. Ray, P. Sadhukhan, K. Naskar, G. Lal, R. Bhar, *et al.*, Polyaniline-multiwalled carbon nanotube (PANI-MWCNT): Room temperature resistive carbon monoxide

(CO) sensor, *Synth. Met.*, 2018, **245**, 182–189, DOI: 10.1016/j.synthmet.2018.08.024.

69 S. H. Nasresfahani, Z. Zargarpour, M. H. Sheikhi and S. F. Nami Ana, Improvement of the carbon monoxide gas sensing properties of polyaniline in the presence of gold nanoparticles at room temperature, *Synth. Met.*, 2020, **265**, 116404, DOI: 10.1016/j.synthmet.2020.116404.

70 C. Liu, Z. Noda, K. Sasaki and K. Hayashi, Development of a polyaniline nanofiber-based carbon monoxide sensor for hydrogen fuel cell application, *Int. J. Hydrogen Energy*, 2012, **37**(18), 13529–13535, DOI: 10.1016/j.ijhydene.2012.06.096.

71 J. Zhao, G. Wu, Y. Hu, Y. Liu, X. Tao and W. Chen, A wearable and highly sensitive CO sensor with a macroscopic polyaniline nanofiber membrane, *J. Mater. Chem. A*, 2015, **3**(48), 24333–24337, DOI: 10.1039/C5TA06734K.

72 A. Sunilkumar, B. S. Khened, B. Chethan, V. Prasad, M. G. Kotresh, T. M. Sharanakumar, *et al.*, Ultrahigh sensitive and selective room temperature operable poisonous carbon monoxide gas sensor based on polyaniline ternary composite, *Inorg. Chem. Commun.*, 2023, **150**, 110476, DOI: 10.1016/j.inoche.2023.110476.

73 A. Jain, M. Dhonde, A. Soni, A. Kumar and K. Sahu, Polyaniline based blends and composites for gas sensing: A comprehensive review on materials, mechanisms, and applications, *React. Funct. Polym.*, 2026, **220**, 106610, DOI: 10.1016/j.reactfunctpolym.2025.106610.